Kelly, J.F.; Barnes, P.; Fisher, G.R. (1995) The use of synchrotron edge topography to study polytype nearest neighbour relationships in SiC. *Radiation Physics and Chemistry* **45** (3): 509-522.

THE USE OF SYNCHROTRON EDGE-TOPOGRAPHY TO STUDY POLYTYPE NEAREST NEIGHBOUR RELATIONSHIPS IN SiC

J F Kelly , P Barnes, G R Fisher

ABSTRACT

A brief review of the phenomenon of polytypism is presented and its prolific abundance in Silicon Carbide discussed. An attempt has been made to emphasise modern developments in understanding this unique behaviour. The properties of Synchrotron Radiation are shown to be ideally suited to studies of polytypes in various materials and in particular the coalescence of polytypes in SiC. It is shown that with complex multipolytypic crystals the technique of edge topography allows the spatial extent of disorder to be determined and, from the superposition of Laue type reflections, neighbourhood relationships between polytypes can be deduced. Finer features have now been observed with the advent of second generation synchrotrons, the resolution available enabling the regions between adjoining polytypes to be examined more closely. It is shown that Long Period Polytypes and One Dimensionally Disordered layers often found in association with regions of high defect density are common features at polytype boundaries. An idealised configuration termed a "polytype sandwich" is presented as a model for the structure of SiC grown by the modified Lely technique. The frequency of common sandwich edge profiles are classified and some general trends of polytype neighbourism are summarised.

INTRODUCTION

Considerable effort has been expended in attempting to understand the origin of the phenomenon of polytypism since its discovery now nearly 90 years ago. The word "polytypie" was first used by Baumhauer (1912) to describe the ability of a material to crystallize into structural modifications differing in only one crystallographic direction. Schneer (1955) called it "polymorphism in one dimension" in order to emphasise that two dimensions of the unit cells of different polytypes are identical whilst the third is a variable integral multiple of a common unit. The polytypic structures thus built up may be considered as stacked layers with repeat sequences ranging from 2 layers to many hundreds of layers (Figure 1); in the extreme case of no finite repeat the polytype can be termed a one dimensionally disordered layer.

Several theories have been put forward to explain the phenomenon notably the screw dislocation theory by Frank (1949) and its later derivatives by Burton, Cabrera & Frank, (1951), Mitchell (1957), Krishna & Verma (1965). The faulted matrix model of Pandey & Krishna (1975 a, b, 1978) and the one dimensional disorder theory of Jagodzinski (1954 a, b) are amongst them. An exhaustive description of polytypism in crystals is given in the review articles by Verma and Krishna (1966), Trigunayat and Chadha (1971) and Pandy & Krishna (1983) summarising the status of understanding of the origin and growth of polytype structures while Schaffer (1969) lists known polytypes and their discoverers.

ON THE ORIGINS OF POLYTYPISM

Early Theories

As early as 1912 Baumhauer tried to correlate the occurrence of various polytypes in SiC crystals with their colour: Hayashi (1960) summarised that green crystals were characteristic of the 6H polytype, yellow of 15R and dark black of 4H. The notation used here is after Ramsdell (1945). Three other common notations due to Haag (1943), Zhdanov (1945, 1946) and Jagodzinski (1949) have also been used to denote the layer (ABC) stacking sequences as shown in Table 1 and discussed more fully by Verma and Krishna (1966).

Jagodzinski	Ramsdell	Hagg	Zhdanov	Sequence
khkh	4H	++--	22	ABAC
hkkhkk	6H	+++---	33	ABCACB
$(kkhkh)_3$	15R	$(++---)_3$	$(23)_3$	ABCBACABACBCACB

TABLE 1: The various notations used to classify polytypes and as applied to the three most common types. The h,k notation used by Jagodzinski describes alternative successive rotations of zero and 180 degrees respectively of one layer with respect to its neighbour; the Ramsdell notation signifes the c-axis repeat and lattice type (H-hexagonal, R-rhombohedral); Hagg counts as + the moves A-B,B-C,C-A and as - the moves A-C,C-B,B-A and lists the consecutive + or - signs; while Zhdanov sums the number of like signs used in the previous notation.

Several workers have reported various findings on the role of impurity content on polytype stability, notably Hayashi (1960) Knippenburg (1963) and Loubser et al (1969). On the other hand Jagodzinski (1954 a, b) developed thermodynamic arguments to account for the existence of polytype behaviour, giving agreement with the known abundancies of various polytypes. Meanwhile Frank (1949) proposed the first explanation based on definite principles of crystal building; this screw dislocation theory has been fully discussed by Verma and Krishna (1966). It has acquired experimental support with the observation of growth spirals by Amelinckx (1951) which have been confirmed by Verma (1951) using phase contract microscopy however it is not easily reconciled with the observation of polytype coalescence. The faulted matrix model proposed by Pandey and Krishna (1975 a, b) considered all polytypes to be some variation on a basic structure (4H, 6H and 15R) generated by stacking faults and as such represents the synthesis of improvements to the dislocation model. Yet despite another model, the periodic slip process due to Mardix et al (1968), no single theory has been so far able to fully account for the presence of all known polytypes.

The obvious difficulty in characterising polytypes of a given compound are their commonly found large unit cells and the enormous number of possible stacking sequences for a given period.

Modern Status

Bogdan and Alexander (1989 a, b) have discussed computer algorithm techniques for generating layer sequences of polytypes and simulated random stacking faults in close packed structures. Monte Carlo computer simulations using different mechanisms for layer rearrangement with periodicities extending to 12 layers have been discussed by Ramasesha and Rao (1977), while Ramasesha (1984) discusses a competing interaction model in terms of the large number of known polytypes and one dimensional disorder based on the Ising spin model The nearest neighbour interaction in this model is ferromagnetic while the next nearest neighbour is antiferromagnetic, the whole system is considered anisotropically. The Monte Carlo method has also been used by Kabra and Pandey (1989) to simulate the 2H to 6H transformation above 1600 ^{o}C where stacking faults are introduced in a random space and time sequence. While recently Farkas-Jahnke (1994) has used the novel approach of using Fibonnaci chains to generate the layer sequences frequently found in faulted ZnS polytypes.

A simpler method devised by Inoue (1982) has produced 20 layer sequences of SiC polytypes by considering the Zhdanov symbol notation. Computer simulations have also been used by Goodby et al (1990) in determining the energies of ZnS and SiC polytypes. Cheng et al (1988) have used ab initio pseudo potential techniques to calculate the energies of SiC polytypes while yet further work by these authors (Cheng, Needs et al. 1989) on determining the Hamiltonian of an Ising spin array have concentrated on an inter layer interaction model. According to their work they find that the observed polytypes of SiC are roughly 0.01 eV per pair of SiC atoms lower in energy than the polytypes that are not seen in experiments.

A superlattice model of polytype formation with different degrees of disorder has recently been formulated by Kozielski and Tomaszewicz (1993) based on $Zn_{1-x}Cd_xS$ while work on Order-Disorder (O-D) structures to include MDO (Maximum Degree of Order) polytypes has been discussed by Durovic (1993). Previously Zvyagin (1988) has considered the relationships of polytype structures to hybrid (both commensurate & incommensurate), Order-Disorder (O-D) and modulated structures in attempting to describe the structural aspects of polytypism. More recently Zvyagin (1993) has summarised the modern status of polytypism with emphasis on the nomenclature and the significance of the structural units (SU) used to describe it.

The foregoing attempts at explaining polytypism have relied upon layer sequencing methods with little regard to experimental observation of polytypes from bulk, thin film or surface measurements. The most recent review of experimental methods to identify polytypic transformations in SiC by Jepps and Page (1984) summarises optical polarisation, X-ray diffractrometric and electron microscopic techniques.

CRYSTALLOGRAPHIC METHODS TO STUDY POLYTYPES

General Methods

The range of polytypic materials that have recently been studied using X-ray diffraction methods includes Cd Br_2 doped CdI_2 dendritic crystals (Kumar and Trigunayat 1993) and Pb doped $CdBr_2$ (Singh and Trigunayat 1993) while the structure determination in particular of SiC polytypes using monochromatic c-axis

oscillation X-ray diffraction has been fully discussed by Verma and Krishna (1966). Although these methods yield the total polytype content of a crystal it is not possible to determine the order of adjacent "neighbouring" polytypes along the crystal c-axis (Figure 2).

To understand this it may be convenient to consider what one may expect to observe with the c-axis oscillation technique: a given low period polytype is relatively easy to index as the cell repeat reflections are inversely proportional to the reciprocal lattice spacing; ie the measured spacing along Bernal rows. However with the superposition of long period polytypes which appear on the photograph as closer spaced reflections between the low period polytype, but without the added information from the morphology and hence distribution of these polytypes with respect to each other within the crystal, it is not possible to locate their exact position. Another problem identified by Golightly and Beaudin (1969) is the exact location of disorder that is present in the crystal as the streaking produced on Laue transmission photographs appears to overlap the discrete reflections from the polytypes.

X-ray transmission Topography also suffers from this limitation to reveal only the quantitative rather than the qualitative polytype content of a crystal as has been discussed by Kelly, Barnes and Fisher (1993). X-ray Topographic techniques in general have long been used, for example by Lang (1959), to study crystal defects and have been successfully employed using Synchrotron Radiation (Fisher and Barnes 1984; Fisher, Barnes & Kelly 1993) in studies of defects in polytypic SiC.

The potential of a Synchrotron Radiation Source (SRS) in imaging polytypic materials derives from: a low beam divergence thus accommodating mixed crystals with high resolution; a wavelength continuum making alignment trivial; high flux enabling rapid data collection, all of which have been summarised by Moore (1994). Several geometries have been employed for various materials; that due to Mardix, Lang, Kowalski and Makepeace (1987) being particularly useful for ZnS crystal whiskers, whilst the **edge geometry** due to Fisher and Barnes (1984) is well suited to SiC platelets and is shown in Figure 3.

Synchrotron Edge Topography

The technique of Synchrotron Edge Topography first used by Fisher and Barnes (1984), discussed by Fisher (1986), summarised by Fisher and Barnes (1990), extended by Barnes, Kelly and Fisher (1991) and reviewed by Kelly, Barnes and Fisher (1993) is now more fully discussed.

The three most commonly found polytypes in SiC are 6H, 15R and 4H, and are shown in Figures 4 and 5. These edge topographs have been indexed using the computer programme WRIST (White Radiation Indexing of Synchrotron Topographs) developed by Fisher and Barnes (1984).

The SiC crystals in general contain a combination of polytypes in syntactic coalescence, which result in an array of superimposed Laue type reflections from the various polytypes. Since all polytypes are visible in (hk. O) reflections they contain information from the whole crystal. By comparing l = 0 reflections the contributions from these reflections to the total crystal thickness may be determined. An example of this is given in Figure 6 of a mainly 6H polytype containing a thinner 4H contribution (sample J13). From a measurement of the thicknesses of the individual polytypes one

finds that these do not always add up to the total crystal thickness (even after allowing for the effect of oblique viewing) indicating quite clearly that layer(s) without a crystallographic repeat in the c-direction must also be present, i.e. one dimensional disorder. A good example of this phenomenon is given in crystal number J59.

With the advent of second generation synchrotrons and the improved resolution obtained by the authors with the preferred edge geometry for SiC more accurate measurements of the polytype thicknesses are now possible and new features have been observed at the polytype boundaries. Thus by projecting each polytype layer on to a common l = 0 position, one can "re-build" the polytypic crystal so that "missing layers" can be confidently assigned a long period polytype (LPP) or, in the case of no finite repeat to one-dimensional disorder (1DD) status. In the former case one would expect to be able to find finely spaced feint reflections (the spacing is inversely proportional to the c-repeat distance) with an identical thickness to the missing layer. The latter case would be a more extreme example of this in which no repeat is observed but rather streaking along the c-direction, as shown in Figure 7.

Long period polytypes (LPP's) and one-dimensionally disordered (1DD) layers are often accompanied by regions of darker contrast in 4150 and 5270 central reflections indicating regions of high defect density confined within a thin layer. These so called defect density bands have been found by Barnes, Kelly and Fisher (1991) to be common features in SiC grown by the modified Lely technique (Lely, 1955). Their observation has also been significantly aided by the improved resolution of second-generation synchrotrons (see Appendix).

POLYTYPE NEIGHBOURHOOD RELATIONSHIPS

As noted above, the use of edge-topogrophy to accurately assign and locate individual LPP/1DD layers enables us to assemble unambiguous models of the whole crystal preserving exact location of each individual layer with respect to each other. Using this methodology a large number of SiC crystals have now been fully classified, this representing a quite unprecedented database on "*polytype neighbourism*". Some of the models derived are quite complex: by way of an example Figure 8 shows a rather unusual case found amongst the crystal sample can be found, which has been termed a "doubly filled sandwich" (see Table 2).

In search of a polytype neighbourhood classification scheme

This complex example can be completely described in terms of *polytype neighbourism* as a 6-layered 6H+6H+1DD+LPP+15R+6H crystal, where the term *doubly filled* refers to the 1DD and LPP layers sandwiched between the shorter period basic polytypes. In this case a 70 μ m thick 1DD layers adjoins a 78H/234R LPP previously reported by Mitchell (1954).

Such descriptions have now been assigned to all 135 (July 2000) crystals in the currently compiled database. However, in looking for statistical trends in *polytype neighbourism* one also needs an effective broad classification scheme. Such a scheme has been prompted by the preliminary observations of Fisher and Barnes (1990) where an analogy was made to everyday varieties of sandwiches; One hundred and nine crystals later the analogy, and its implied set of rules, still hold and so this

classification scheme has been developed further for this study as will now be explained.

The authors in attempting to rationalise the different nearest neighbour polytype arrangements found have identified 6 types of polytype sandwiches and 3 multi-polytype layer configurations as possible models of vapour grown SiC. A schematic illustration of this classification, used for the SiC database, is shown in Figure 9.

The failure, on systematic searching, to find a single occurrence of the reverse sandwich has prompted the authors to consider this absence to be a fundamental rule of SiC polytypism, and they have speculated (Fisher & Barnes, 1990) on possible reasons for this. This situation can be contrasted to that of the tautological "empty sandwich" (ie no filling) or multi-polytype crystal as it will be referred to from here on (see Figure 9).

In the case of the double polytype crystal, composed of basic 6H, 4H and 15R layers, only two of the three possible permutations (6H+4H; 6H+15R) have been found to exist in practice. Nevertheless the basic polytypes 4H and 15R can exist as an asymmetric sandwich when there is an intervening layer filling, either LPP or 1DD,present invariably accompanied by a region of high defect density. So clearly there is no prohibitive rule here analogous to the reverse sandwich rule; rather a corollary to the observed occurrence of single poltypes and open sandwiches.

Statistical Trends and Rules of Neighbouring Polytypism

These considerations have led the authors to present the abundancies of the various polytype models into a statistical table (see Table 2). From this it is clear that the predominant growth pattern in SiC is the complex multi- polytype sandwich layering sequence. Over half of all the crystals display a complex pattern of more than one polytype in syntactic coalescence in combination with a variety of LPP repeats and/ or 1DD layers between them.

SANDWICH	**Reverse**	**Simple**	**Asymmetric**	**Open**	**Doubly-filled**	**American Club**
NUMBER	0	15	26	7	4	36
POLYTYPE		**Single**	**Double**			**Multi**
NUMBER		8	6			7

TABLE 2: Statistical trend of various polytype occurrences classified according to the scheme of figure 8 obtained from the survey of 109 crystals.

It is interesting to note that of the crystals that have formed as single polytypes all have been of the basic 6H structure. No single polytypes of the 4H or 15R structure have so far been observed. So while double polytypes of the 6H+15R and 6H+4H structure have been recorded in the approximate ratio 2:1 the occurence of the double polytype 4H+15R might seem less likely. This indeed is the case. On this basis it is also not surprising that of all the simple sandwiches measured (this forms part of a larger survey detailing the LPP repeats, documenting the defect band boundaries and

measuring the size of the 1DD layers) they have consisted only of the 6H+1DD/LPP+6H type.

Approximately 80% of the crystals surveyed contain planes of high defect density in the regions between adjoining polytypes or contain disordered layers ranging from 5μ m to about 300 μ m (with a resolution limit of +/- 2.5 μ m). While generally the majority of these are thin layers less than about 20 μ m in size. These are an exceptionally common occurrence in the class of models termed asymmetric, doubly filled, open and American club sandwiches, and appear against and between all of the triple 6H,4H,15R polytype configurations. Not surprisingly, of the combination orders possible (6H+4H+15R; 6H+15R+4H; 4H+6H+15R), all are found to exist: this lack of any preference then appears to result from the presence of the thin defect layers ("defect bands") which can act to separate two polytypes which cannot syntactically coalesce. It is striking to note that in between all occurrences of adjoining 4H and 15R polytypes there always appears to be either a LPP or 1DD layer or a band of high defect density that we believe acts to accomodate any apparent mismatch between the two lattices resulting from the change in periodicity of the polytypes. Such layers do not correlate only just with polytype changes since they can also occur even within a region of the same polytype. It is of course possible that a defect band between two regions of the same polytype is a reminiscence of a previous state where one of the the surrounding polytypes was once different (prior to transformation) though this can only be speculation.

This survey has clearly highlighted the ubiquitous nature of the sandwich configuration in the formation of SiC polytypes along with the prescence of highly defective layers. These points are now discussed further.

CONCLUSIONS

The general description of the pattern of polytype distribution within SiC can be summarised as follows:

1 Complex sandwich arrangements provide the majority of polytype models of SiC.

2 Thin high defect density bands (down to = 5 μ m thickness) exist at many of the boundaries between polytype-polytype and polytype-disordered layers.

3 Only the basic 6H polytype appears as a *stand-alone* polytype.

4 The 4H and 15R neighbours have always been found to be separated by LPP, 1DD or defect layers.

5 The reverse sandwich configuration has so far still not been observed.

These rules pose some implications concerning the growth and stability of various polytypes. No definitive evidence has so far been found to show whether complex polytype combinations are formed during growth or by post- growth transformation or by some combination of both scenarios. Either way, the ubiquitous nature of the LPP/1DD and defect band layers appears to be signalling some message concerning growth mechanisms: given the near- impossibility of performing in-situ time-resolved topographgy at ~2,000 C, one must make the most of these post-growth clues. One

can speculate that if post-growth transformations occur, these thin layer combinations remain as a condensation of defects and mismatch strains from the whole polytype; that is transformation commences at the opposite boundary and then spreads towards the transition boundary leaving an ever-decreasing layer containing the former polytype; this layer will have collected the defects and mismatch strain into a very thin region, sometimes to the point of becoming one-dimensionally disordered. In the other growth scenario, where a new polytype starts to grow on its substrate due to changing temperature/vapour-saturation conditions, the thin LPP/1DD/defective layer presumably acts as a thin transition layer to nucleate the growth of the new polytype and keep defects and mismatch strain largely removed from the two adjacent stable polytypes.

Of these two scenarios, the post-transformation mode seems the more plausible explanation for the common occurrence of these thin layers. Either way their presence appears to adequately explain some of the statistical trends in polytypism. For example, within the three most common SiC-polytypes, 6H, 4H and 15R, one might have expected some statistical neighbourhood preference between these polytypes representing the relative ease of one of these polytypes against another to be adjacent to a third polytype. However the survey shows that syntactic coalescence only appears to exist against the 6H-polytype, thin intervening layers separating other combinations. Not surprisingly then throughout the simultaneous occurrences of 6H, 4H, 15R there is no real preferred order, all three permutations (6H+4H+15R; 4H+6H+15R; 6H+15R+4H) occurring.

The common presence of LPP/1DD/defective layers thus partly explains the prolific abundance of polytypes in silicon carbide and in particular the rich variety of complex multi-polytype and sandwich combinations. True syntactic coalescence only appears to exist with the 6H-polytype and this appears to mark the 6H-polytype, which is also the most abundant polytype in the survey, as a more fundamental polytype structure.

Finally one notes that the previous observation by Fisher and Barnes (1990), that reverse sandwiches never exist, still remains 100% intact after some one hundred and nine cases of depth-profiling. This observation cannot really be used to differentiate between alternative modes of growth (see Fisher and Barnes, 1990) but it certainly demonstrates the greater stability of short order polytypes at lower temperatures. Taking into account all the observations, one concludes that the order of stability conforms to 6H > 4H, 15R > LPP, 1DD.

ACKNOWLEDGEMENTS

Daresbury Laboratory Synchrotron Radiation Source and associated personnel (station 7.6); EPSRC for synchrotron beam time.

REFERENCES

Amelinckx S. (1951) Nature **16**7, 939

Barnes P., Kelly J.F. and Fisher G.R. (1991) Phil. Mag. Lett. **64**, 7-13

Baumhauer H. (1912) Z. Krist. **50**, 33-39

Bogdan N. and Alexander B. (1989a) Phase Transitions **16/17**, 549-553

Bogdan N. and Alexander B. (1989b) Phase Transitions **16/17**, 555-559

Burton W.K., Cabrera N. and Frank F.C. (1951) Trans. Roy. Soc. **A243**, 299-358

Cheng C., Needs R.J., Heine V. and Jones I.L. (1989) Phase Transitions **16/17**, 263-274

Cheng C., Needs R.J. and Heine V. (1988) J. Phys. C **21**, 1049-1063

Durovic S. (1993) Phase Transitions **43** (1-4), 81-87

Farkas-Jahnke M. (1994) Materials Science Forum **150-151**, 65-76

Fisher G.R., Barnes P. and Kelly J.F. (1993) J. Appl. Cryst. **26**(5),677

Fisher G.R. and Barnes P. (1990) Phil. Mag. **B61**, 217-236

Fisher G.R. (1986) Ph.D Thesis, University of London

Fisher G.R. and Barnes P. (1984) J. Appl. Cryst. **17**, 231-237

Frank F.C. (1949) Discuss. Faraday Soc. no.5, 48-54

Gasilova E.B. (1955) Dolk. Akad. Nauk SSSR **101**, 671

Golightly J.P. and Beaudin L.J. (1969) Mat. Res. Bull. (Proc. Int. Conf. on SiC) **4**, 119128

Goodby R., Needs R.J. and Payne M. (1990) Physics World **3** no.10, 39-43

Haag G. (1943) Arkiv. fur Kemi. Mineralogi och Geologi **16B**, 1-6

Hayashi A. (1960) J. Mineral. Soc. Japan **4**, 363-371

Inoue Z. (1982) J. Mat. Sci. **17**, 3189-3196

Jagodzinski H. (1954a) Neues Jb. Miner. Monatsh. **3**, 49-65

Jagodzinski H. (1954b) Acta Crystallogr. **7**, 300

Jagodzinski H. (1949) Acta Crystallogr. **2**, 201-207

Jepps N.W. and Page T.F. (1984) J. Prog. Cryst. Growth Charact. **7**, 259-307

Kabra V.K. and Pandey D. (1989) Phase Transitions **16/17**, 211-229

Kelly J.F., Barnes P. and Fisher G.R. (1993) Phase Transitions **43**(1-4), 137-143

Kozielski M.J. and Tomaszewicz A. (1993) Phase Transitions **43** (1-4),

Knippenburg W.F. (1963) Phillips Res. Rept. **18**, 161-274

Krishna P. and Verma A.R. (1965) Z. Krist. **121**, 36-54

Kumar B. and Trigunayat G.C. (1993) Phase Transitions **43**(1-4),

Kuo Chang-Lin (1965) Acta. Phys. Sinica **21**, 1089

Lang A.R. (1959) Acta Cryst. **12**, 249-250

Lely J.A. (1955) Ber. Deutsch. Keram. Ges. **32**, 229-231

Loubser J.H.N., De Sousa Balona J.A. and Van Ryneveld W.P. (1969) Mat. Res. Bull. (Proc. Int. Conf. on SiC) **4**, S249-S260

Mardix S., Lang A.R., Kowalski G. and Makepeace A.P.W. (1987) Phil. Mag. A **56**, 251-261

Mardix S., Kalman Z.H. and Steinberger I.T. (1968) Acta Crystallogr. A **24**, 464-469

Mitchell R.S. (1957) Z.Krist. **109**, 1-28

Mitchell R.S. (1954) J. Chem. Phys. **22**, 1977

Moore M. (1994) Radiat. Phys. Chem. **45**, 427-444

Pandey D. and Krishna P. (1983) Prog. Cryst. Growth Charact. **7**, 213-257

Pandey D. and Krishna P. (1978) Advances in Crystallography Oxford and IBH,New Delhi

Pandey D. and Krishna P. (1975a) J.Cryst. Growth **31**, 66-71

Pandey D. and Krishna P. (1975b) Phil. Mag. **31**, 1113-1148

Price G.D. and Yeomans J.M. (1988) Proc. CMS workshop Los Alamos Springer Verlag,p60

Ramasesha S. (1984) Pramana (India) **23** no.6, 745-749

Ramasesha S. and Rao C.N.R (1977) Phil. Mag. **36** no.4, 827-833

Ramsdell L.S. and Kohn J.A. (1952) Acta. Cryst. **5**, 215-224

Ramsdell L.S. (1945) Am. Mineral. **32**, 64-82

Schaffer B.T. (1969) Acta. Cryst **B25**, 477-488

Schneer C.J. (1955) Acta Cryst. **8**, 279285

Singh and Trigunayat (1993) Phase Transitions **43**(1-4),

Smith J., Yeomans J.and Heine V. (1984) NATO ASI Series E **83**, 95-105

Trigunayat G.C. and Chadha G.K. (1971) Phys.Stat. Sol.(a) **4**, 9-42

Van Loan P.R. (1967) Am. Min. **52**, 946

Verma A.R. and Krishna P. (1966) Polymorphism and Polytypism in Crystals J.Wiley, New York

Verma A.R. (1951) Nature **168**, 430-431

Yeomans J.M. and Price G.D. (1986) Bull. Mineral. **109**, 3-13

Zhdanov G.S. and Minervina Z.V. (1946) J. Phys. USSR **10**, 422-424

Zhdanov G.S. and Minervina Z.V. (1945) Compt. Rend. Acad. Sci. USSR **48**, 182-184

Zvyagin B.B. (1988) Comput. Math. Applic. **16**, no.5-8, 569-591

Zvyagin B.B. (1993) Phase Transitions **43** (1-4), 21-25

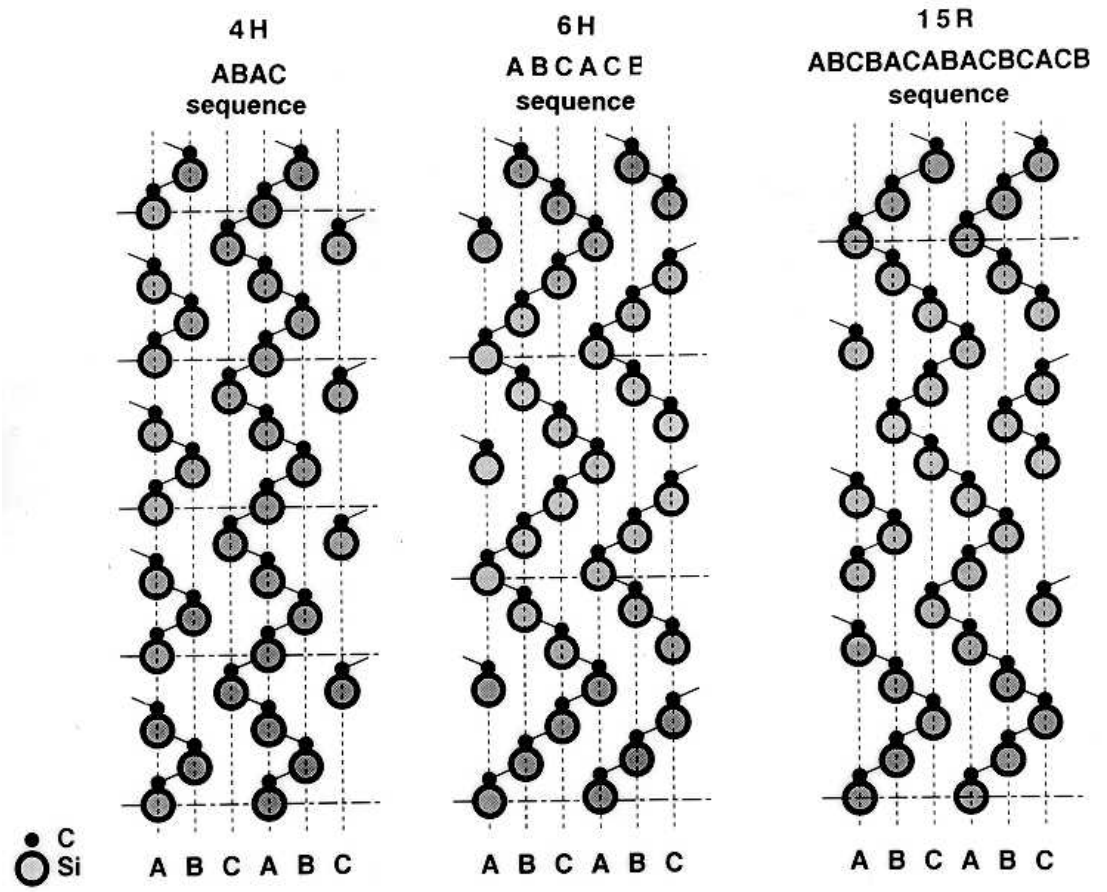

Figure 1. A two-dimensional representation of the 1120 plane in SiC clearly showing the 4H, 6H and 15R stacking sequences, described in Table 1, of the three most common polytypes. The three stacking configurations (A, B, C) are indicated by vertical broken lines and the unit cell repeats by horizontal broken lines. Covalently bonded SiC is essentially a layered material where a spacing of 2518Å between the layers corresponds to a c-axis unit cell repeat of approximately 10Å, 15Å and 38Å respectively for the three cases shown. When the stacking sequence becomes random and there is no finite repeat the layer becomes disordered in one dimension.

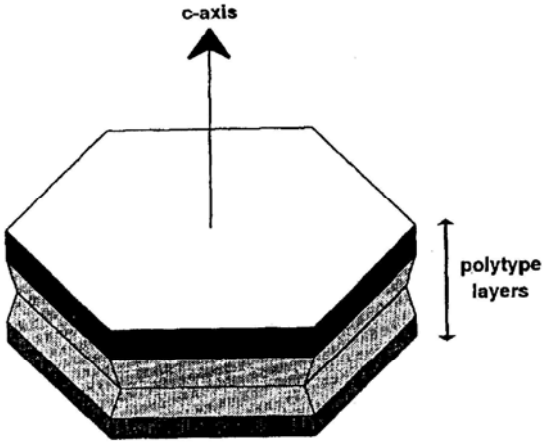

Figure 2. Crystals of SiC grown by the modified Lely technique form hexagonal platelets varying in thickness from about 100μm up to approximately 3mm containing various combinations of polytypes parallel to the crystallographic c-axis as illustrated. The exact locating of these individual polytype layers and their immediate neighbours and intervening regions of disorder has been significantly improved with the advent of synchrotron edge topography schematically depicted in Figure 3.

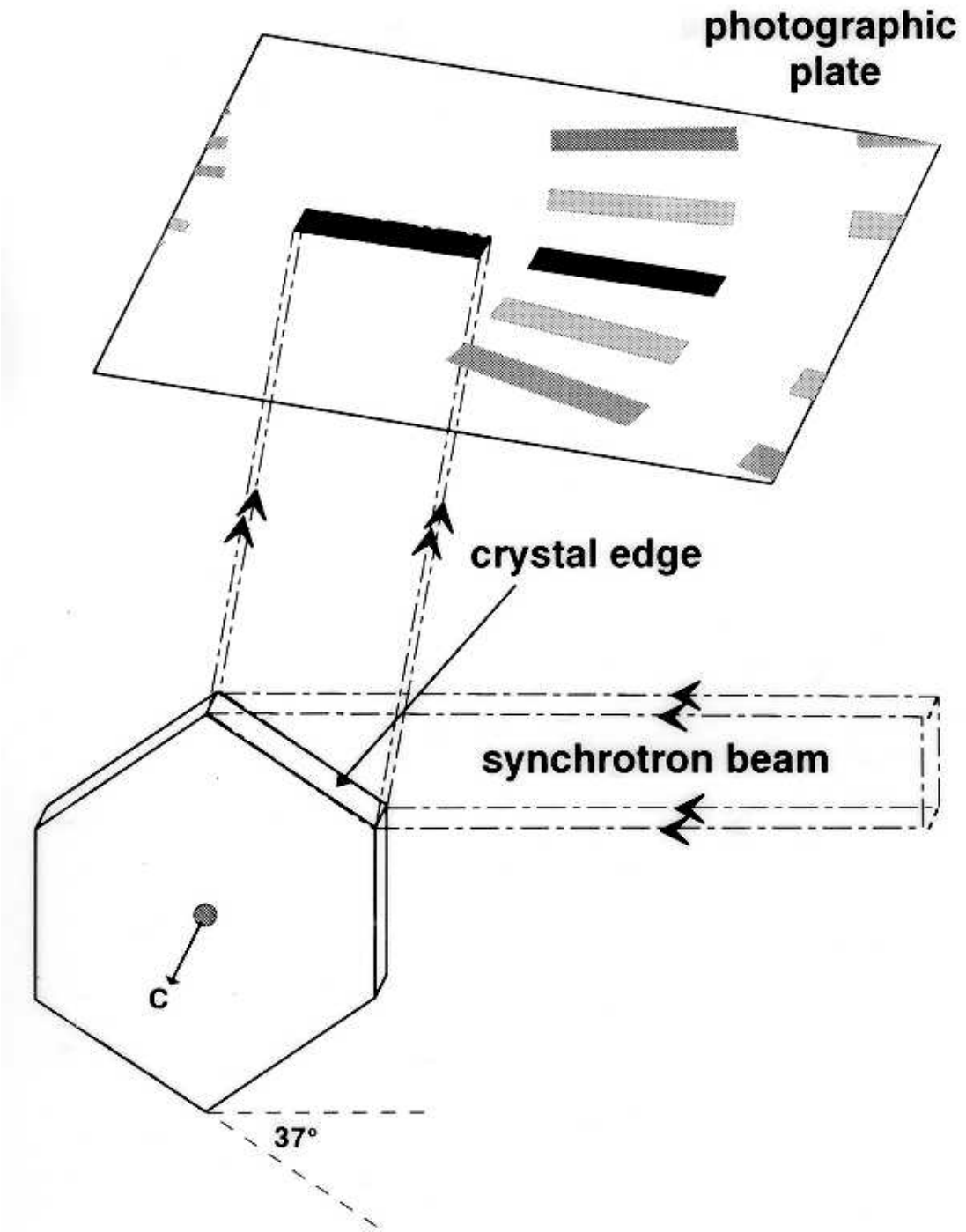

Figure 3. Schematic of the experimental geometry at the SRS, optimised for compromise between image resolution and amount of useful information per photographic plate; used to obtain depth profiles from a SiC crystal edge. Typical dimensions are a source-sample distance ~ 80m and a sample-plate distance ~ 50 mm. The geometry is nominally centered on the 213l row for l = 1.5 Å, 2θ = 100° with the crystal edge inclined at an angle of 37° to the horizontal as shown. Under such conditions the photographic plate will record a Laue type pattern of the crystal. The diagram highlights a central l = 0 reflection topograpgh of the crystal edge (darker type) in which all of the polytypes would be present. In the adjacent row for those reflections when l = 0 different polytypes would be displaced spatially as illustrated (see text for an explanation).

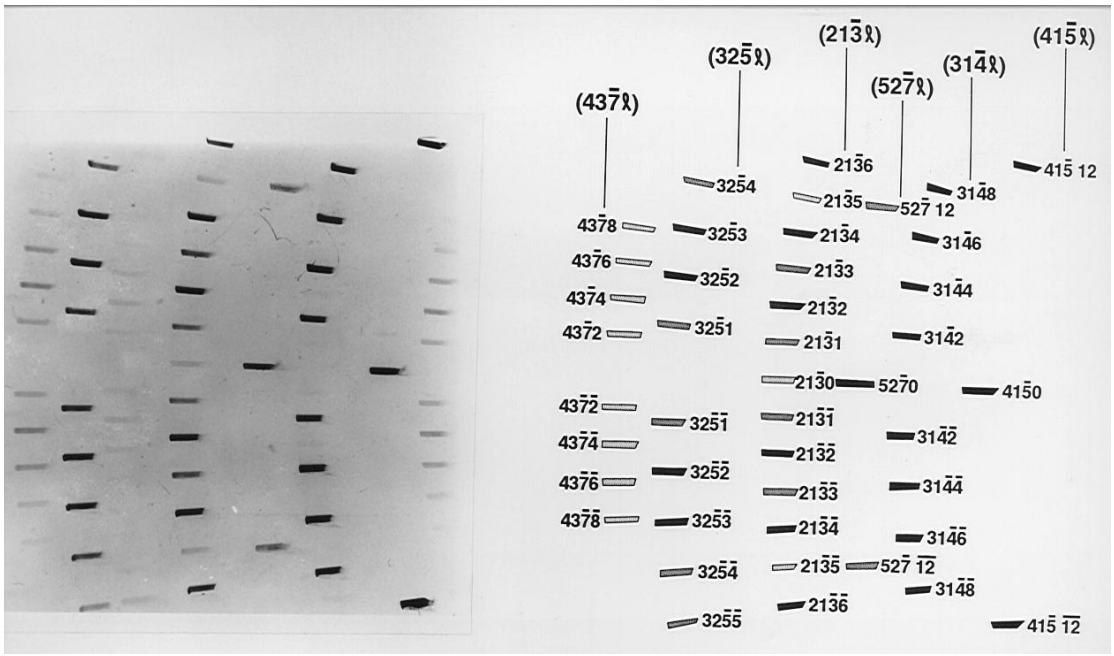

Figure 4. Indexed edge reflections calculated using the computer program WRIST, together with a full plate edge topograph of SiC obtained using synchrotron radiation with the geometry depicted in Figure 3. The fundamental reflections, which have been extensively used in this study, have been indexed using WRIST and correspond in this case to the 6H polytype only (some feint harmonic contributions are also just visible). The plate has been nominally aligned to record the 21$\underline{3}$ ℓ row. The central 52$\underline{7}$0 and 41$\underline{5}$0 reflections provide useful information from all the polytypes present in the crystal, while the authors have taken measurements principally from the 31$\underline{4}$ ℓ row. From such measurements the sample J112, which was topographed prior to the High Brightness Lattice (HBL) upgrade to the SRS and thought to contain only the 6H polytype, has been re-topographed and now reveals with the improved resolution available a 30μm 1DD layer sandwiched between two 6H polytypes. The model for such a crystal has been termed a simple sandwich (see Figure 9).

(Note that all underscores of numbers should be overscores.)

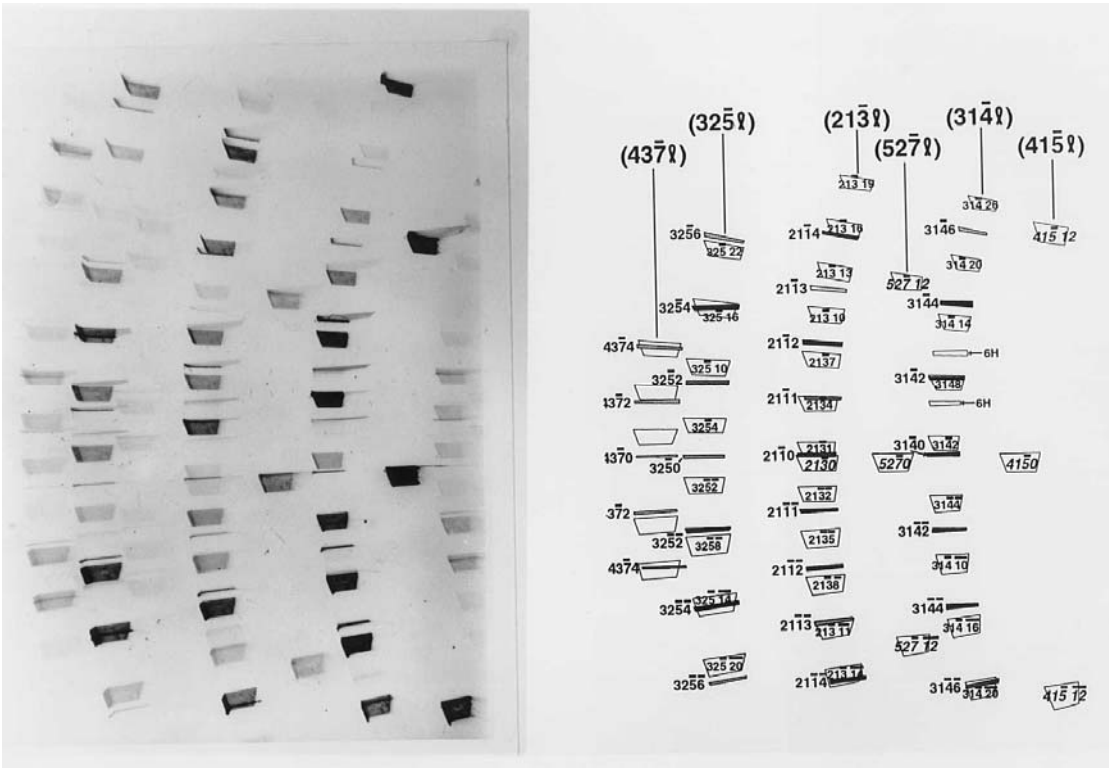

Figure 5. A similar topograph to that in Figure 4 showing the principal indexed reflections of the 15R and 4H polytypes which form the major part of a complex 15R + 1DD + 15R + 1DD + 6H + 1DD + 4H + 6H multipolytypic crystal, sample J14.

For a structure with a rhombohedral lattice, the positions of X-ray diffraction spots are not symmetrical about the zero layer line because the hexagonal unit cell is non-primitive causing the hkl reflections to be absent when - h + k + l is not equal to 3 n (+ or - n = 0, 1, 2 ....). For the 213 l row shown the permitted reflections above the zero layer line are 21.1, 21.4, 21.7 etc. while below this line for bar (-ve) only the reflections 21.2, 21.5, 21.8 etc are visible. The l=0 line will conveniently divide the spots on each side in the ratio 1:2, on visual inspection this allows quick identification of a rhombohedral lattice.

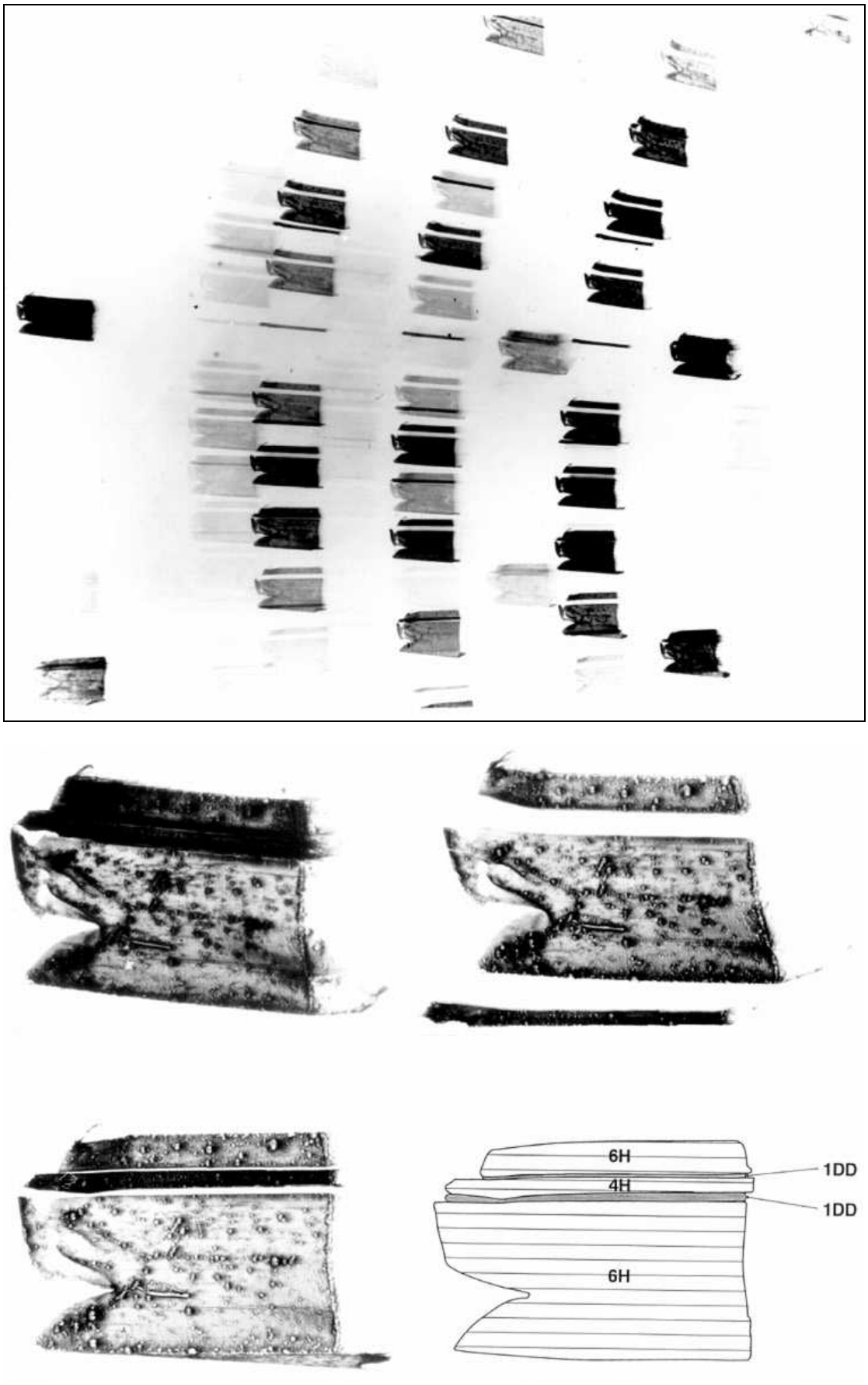

Figure 6. Illustration of the "missing piece" method of assignment for a complex sandwich SiC crystal J13.

(top) A full plate topograph showing the contributions from the basic 6H and 4H polytypes, the pattern is useful in recognising the overlap of the 31$\underline{4}$4 4H reflection with the 31$\underline{4}$6 6H reflection.
(middle left) An enlargement of the central 41$\underline{5}$0 (h, k, l = 0) reflection showing the total crystal profile containing all the polytypes with a measured thickness of 2280 m m. Bands of high defect density can be seen at the boundaries between changing morphology and may indicate the prescence of 1DD layers.
(middle right) An enlargement of part of the 31$\underline{4}$l row showing the spatial displacement of different polytypes along the row. The two parts of the 31$\underline{4}$4 6H reflection show a "missing" piece which may be accounted for by the displaced 31$\underline{4}$2 4H reflection immediately below it. However the individual sizes of the 6H+4H+6H reflections have been measured as 350+170+1680mm respectively totalling 2200mm which leaves 80mm unaccounted for.
(bottom left) An enlargement of the same row containing simultaneously the 31$\underline{4}$6 6H and 31$\underline{4}$4 4H reflections which overlap. In this case (l ¹ 0) unlike the 41$\underline{5}$0 (l = 0) reflection where the whole crystal provides diffraction contrast and there are clearly visible two abscences of contrast corresponding to polytype layers with either a long repeat or with one dimensional disorder. Since the layers are relatively thin » 20 m m and 60 m m, and there are no feint closely spaced reflections suggesting LPP's, the streaking due to disorder would be negligible and the layers have been assigned 1DD status.
(bottom right) A model to scale of the polytypic content of the crystal which for the purposes of this survey has been termed an American club sandwich .

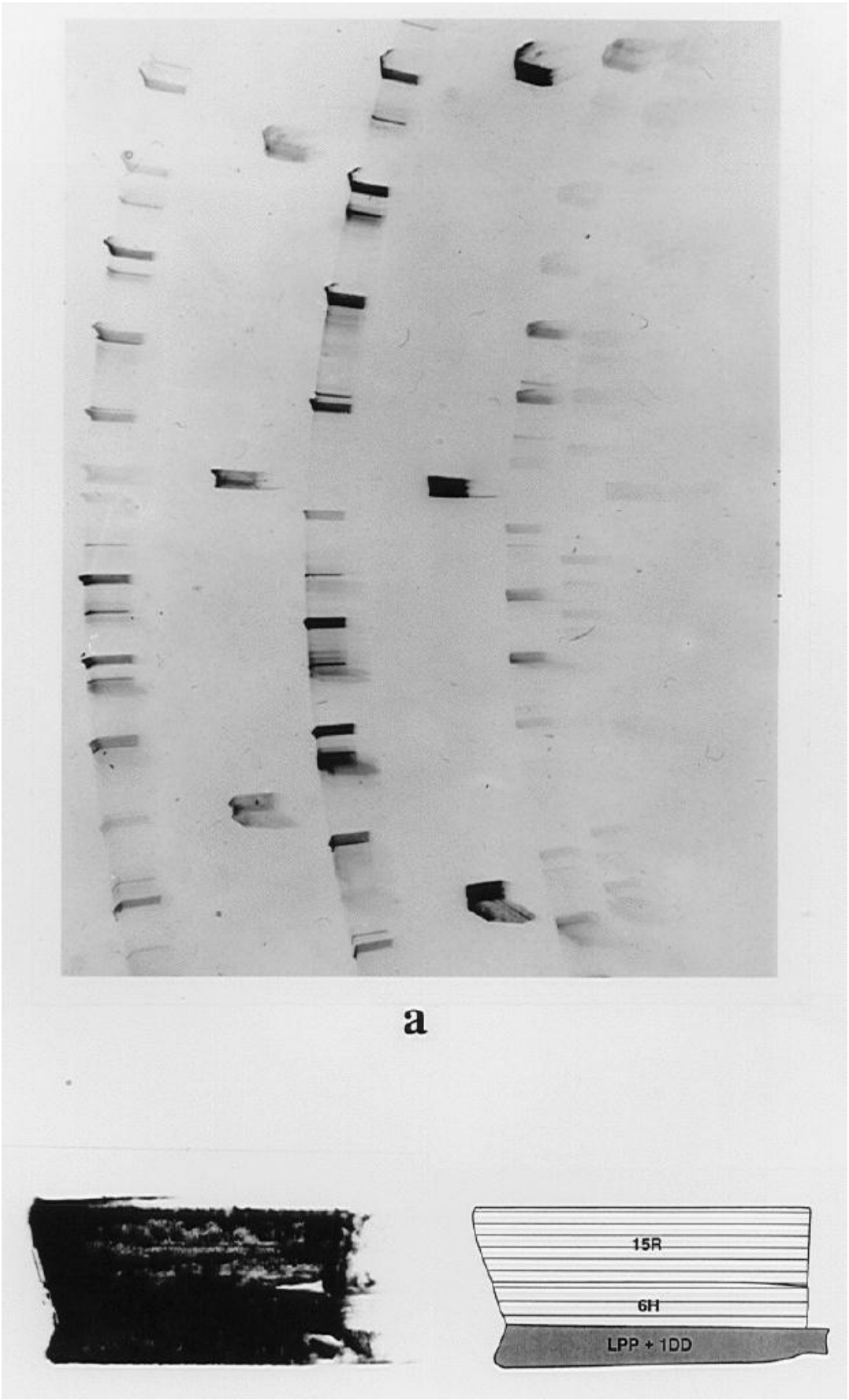

Figure 7. An example of a highly disordered SiC crystal **(J59)**, illustrated by extensive streaking along the diffraction rows.

(a) A full plate topograph containing principally the 6H and 15R polytypes although there are some disordered layers & long period polytypes present. In the former case there is streaking visible along the 31$\underline{4}$l row and in the latter case some feint reflections between the shorter period polytypes. The measured thickness of the 15R and 6H polytype reflections are 530 m m and 120 m m respectively totalling 650 m m.
(b) A 4150 central reflection, containing all the polytypes, has a measured total crystal thickness of 950 m m which can not be accounted for by the 6H and 15R polytypes alone. Heavy defect density bands are also present and are visible at the boundaries between the 15R/6H polytypes and the 6H/LPP/1DD layers. These have been a commonly found occurrence in this survey as is illustrated in table 3.
(c) A model to scale of the measured polytypes and the unaccounted for LPP/1DD layers of ~ 300 m m thickness forming a rarely found open sandwich configuration (see figure 8).

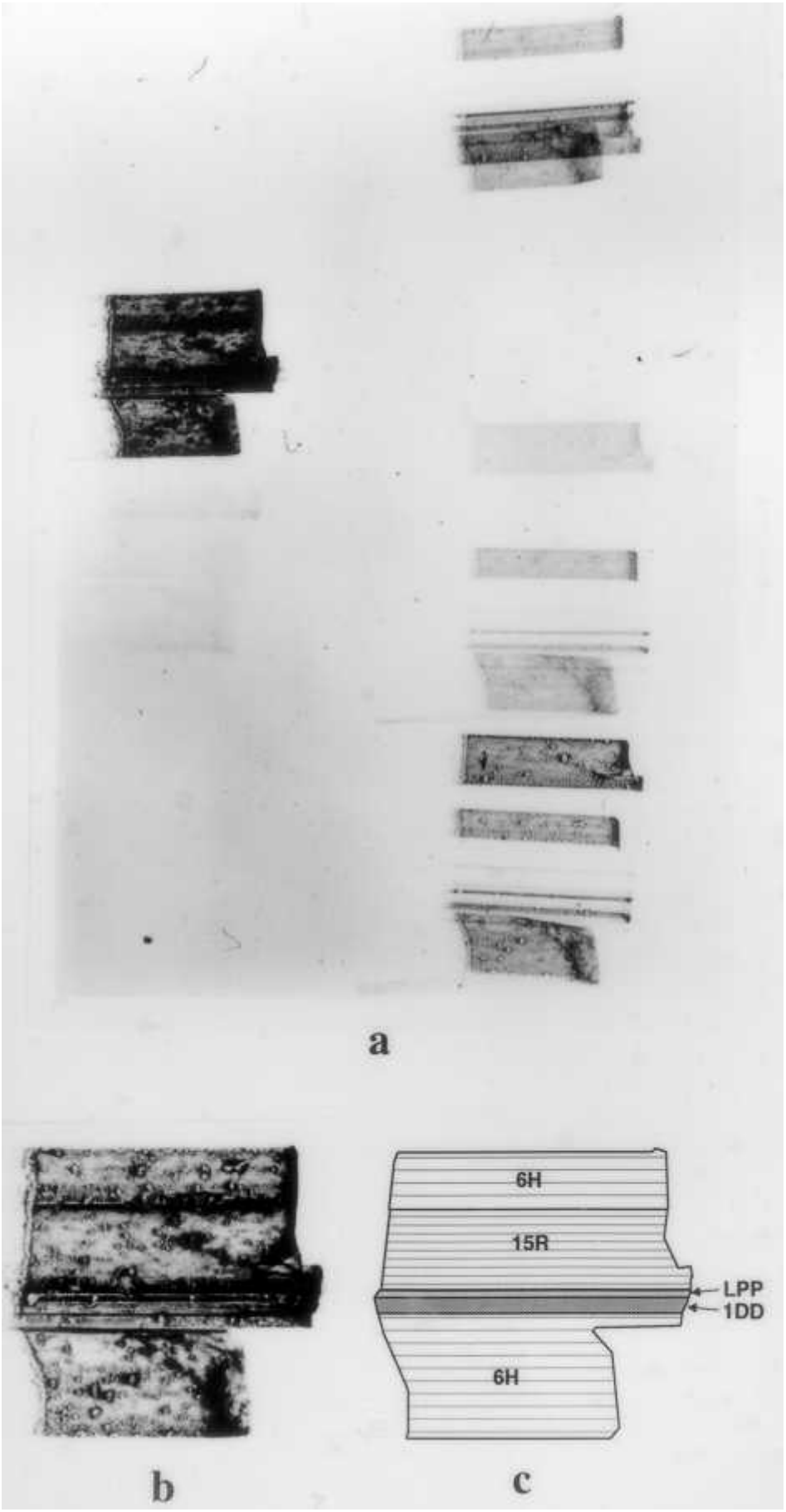

Figure 8. An example of a doubly filled sandwich cofiguration as classified using non-degenerate polytype sandwich scheme.
(a) Part of a full plate edge topograph of a complex array of thick basic poytypes and thinner 1DD/LPP layers forming a doubly filled sandwich that can now be confidently resolved

routinely and adding to the database on polytype neighbourism. The double filling is a 70 m m 1DD layer next to a LPP assigned 78H/234R, previously reported by Mitchell (1954).
(b) The central 41$\underline{5}$0 reflection giving a full crystal thickness of 2550 m m and showing defect density bands at all the polytype-polytype and polytype-disorder boundaries.
(c) A model to scale of the polytypic content of sample J33.

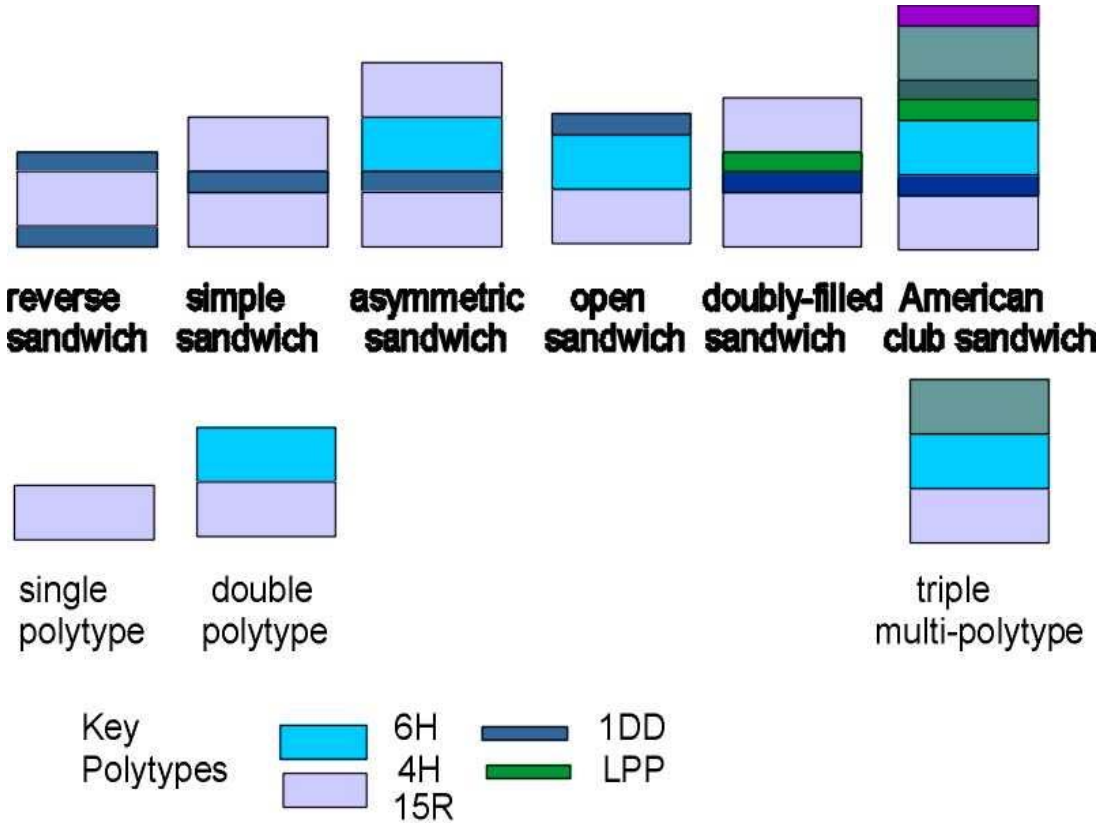

Figure 9. Schematic illustrating the various non-degenerate polytype configurations observed in SiC arranged in order of increasing complexity of model. For convenience the basic common polytypes are shown as vertical and hatched lines while the LPP/1DD regions as darker typeface.
(a) The various sandwiches that have been observed containing LPP/1DD layers as fillings or as an asymmetric layer, in the case of the open sandwich, on only one face of the crystal are shown. It should be noted that No example of the reverse sandwich has been observed in this survey and the authors have included it for completeness.
(b) Multipolytypes of silicon carbide occur in roughly equal proportion in the survey representing approximately 20% of the sample. While only the 6H single polytype has been observed as a stand-alone, combinations of either 4H and/or 15R polytypes syntactically coalesce alongside the 6H to form doubles and triples.

Appendix

Resolution limit in synchrotron topography of SiC

The resolution that can be obtained in single crystal topography experiments using the Synchrotron Radiation Source (SRS) at Daresbury laboratory is governed by geometric considerations and results from the collimation achieved at the 7.6 hutch some 80 metres from the ring. The specimen-photographic plate distance is optimised for the amount of useful high quality topographic information that can be recorded on each glass plate.

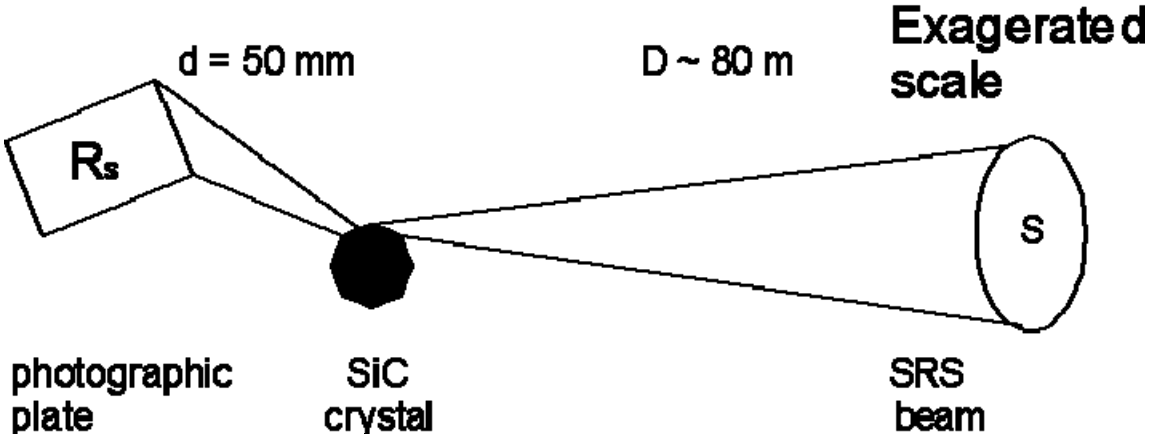

Diagram showing the experimental geometry at station 7.6 of the Daresbury SRS to obtain edge topographs of multipolytypic SiC (resolution R_s in the horizontal plane).

The resolution is governed by the source size S and since the divergence of the beam can be considered to be negligible q_h » 0.01 mrad, the situation illustrated in figure 1 can be described approximately by the following expression:

Where R is the resolution and using some typical values $\frac{R}{d} \cong \frac{S}{D}$

d is the specimen to plate distance, d = 50 mm

S is the source size S = 0.97 mm [(1)]

D is the source to specimen distance D » 80 m

$$R = \frac{0.97 \times 10^{-3}}{80} \times 50 \times 10^{-3} = 0.5 \text{ m m}$$

A comparison of the resolution R in the horizontal and vertical planes for both the pre and post HBL SRS are summarised in the table below. The choice of geometry is governed by a number of factors, that due to Mardix et al [(2)] (vertical alignment) is particularly useful for ZnS whiskers while that due to Fisher & Barnes [(3)] (horizontal alignment) is particularly suited to hexagonal platelets of silicon carbide. [Note the improvement in the horizontal plane]

Table of calculated resolution R in terms of beam size S

Pre-HBL	S(mm)	R (m m)	Post-HBL	S(mm)	R (m m)
horizontal	5.5	3.5		0.97 [(4)]	0.6
vertical	0.29	0.2		0.15	0.09

References

1. M.W. Poole *Personal Communication*

2. Mardix S., Lang A.R., Kowalski G. and Makepeace A.P.W. (1987) Phil. Mag. A **56**, 251-261

3. Fisher G.R. and Barnes P. (1984) J. Appl. Cryst. **17**, 231-237
4. Dobbing G.S. Daresbury Internal Report SRS/APN/98/126